

Magnetic Property Studies of Manganese–Phosphate Complexes

C. V. Krishnamohan Sharma,^{†,§} Charles C. Chusuei,^{*,‡} Rodolphe Clérac,^{†,||} Teresia Möller,[†] Kim R. Dunbar,[†] and Abraham Clearfield[†]

Department of Chemistry, Texas A&M University, College Station, Texas 77842-3012, Alexza Molecular Delivery Corporation, 1001 East Meadow Circle, Palo Alto, California 94303, Department of Chemistry, University of Missouri, Rolla, Missouri 65409-0010, and Centre de Recherche Paul Pascal, CNRS UPR 8641, Av. Dr. A. Schweitzer, 33600 Pessac, France

Received February 6, 2003

Phosphoric acid forms two distinct coordination compounds with manganese salts in aqueous media, a two-dimensional layered structure, $[\text{Mn}(\text{HPO}_4) \cdot (\text{H}_2\text{O})_3]$, **1**, under ambient conditions, and a three-dimensional synthetic mineral, $[\text{Mn}_5(\mu\text{-OH})_2(\text{HPO}_4)_2(\text{PO}_4)_2(\text{H}_2\text{O})_2]$, **2**, under hydrothermal procedures, at 120 °C. In compound **1**, the oxygen atom of the doubly deprotonated phosphoric acid interconnects the metal centers to form a layered structure. The neutral hydrophilic layers of **1** are separated by 5.5 Å and may potentially intercalate hydrophilic organic guest molecules. The metal centers in **2** are octahedral and bridged by PO_4^{3-} , HPO_4^{2-} , and OH_2 groups to form a complex three-dimensional network. XPS analysis on **1** and **2** confirms that manganese exists in the +2 oxidation state. Compound **2** is a poor ion exchanger, but some improvement is observed on partial dehydration. The magnetic properties of both **1** and **2** were studied in detail to examine the amplitude of the magnetic interactions through phosphate ligand bridges. While **1** reveals dominant antiferromagnetic interactions between the spin carriers, a complete investigation of the magnetic properties of **2** revealed its true nature to be a glassy magnet.

Introduction

There has been recent interest in the study of microporous transition-metal phosphate complexes due to their potential applications in catalysis, ion exchange, water-oxidation, magnetism, and coating-lubrication.^{1–4} Efforts to understand coordination and hydrogen-bonding properties of organo-phosphonates with transition metals have resulted in the elucidation of several supramolecular assemblies in our laboratory with interesting ion exchange and magnetic properties.^{5,6} Continuing efforts to understand the issues related to the structural topologies of metal–phosphates (and

phosphonates) have led us to explore the phosphate chemistry of magnetically active metals.⁷ Manganese–phosphates, in particular, exhibit a wide variety of valences (i.e., II, III, IV, and V), the synthetic and structural chemistry of which is relatively unexplored.^{1–3} The oxidation-resistant ligand, PO_4^{3-} , stabilizes high valence manganese complexes in aqueous media and provides convenient routes for the isolation of the bis(μ -oxo)(μ -phosphate) dimanganese (IV, IV) dimer from a solution of the mixed valence (III, IV) dimers in H_3PO_4 . These pathways are important in the study of water-oxidation catalysis in biological processes.² In the presence of 2,2'-bipyridyl and some of the Mn(II) salts formed stable Mn(III–IV) mixed valence complexes with oxo bridges when reacted with phosphoric acid. However, Mn(II) complexes with orthophosphates in aqueous media

* Corresponding author. E-mail: chusuei@umr.edu.

† Texas A&M University.

§ Alexza Molecular Delivery Corporation.

‡ University of Missouri.

|| Centre de Recherche Paul Pascal.

- (1) (a) Brudvig, G. W.; Crabtree, R. H. *Prog. Inorg. Chem.* **1989**, *37*, 99. (b) Christou, G. *Acc. Chem. Res.* **1989**, *22*, 328. (c) Pecoraro, V. L. *Photochem. Photobiol.* **1988**, *48*, 249.
- (2) (a) Sarneski, J. E.; Brzezinski, L. J.; Anderson, B.; Didiuk, M.; Manchanda, R.; Crabtree, R. H.; Brudvig, G. W.; Schulte, G. K. *Inorg. Chem.* **1993**, *32*, 3265. (b) Sarneski, J. E.; Didiuk, M.; Thorp, H. H.; Crabtree, R. H.; Brudvig, G. W.; Faller, J. W.; Schulte, G. K. *Inorg. Chem.* **1991**, *30*, 2835.
- (3) (a) Collins, T. J.; Kostka, K. L.; Uffelman, E. S.; Weinberger, T. L. *Inorg. Chem.* **1991**, *30*, 4204. (b) Collins, T. J.; Gordon-Wylie, S. W. *J. Am. Chem. Soc.* **1989**, *111*, 4511.
- (4) Hivart, P.; Hauw, B.; Bricout, J. P.; Oudin, J. *Tribol. Int.* **1997**, *30*, 561.
- (5) Clearfield, A. *Metal Phosphonate Chemistry*. In *Progress in Inorganic Chemistry*; Karlin, K. D., Ed.; John Wiley & Sons: New York, 1998; Vol. 47, 371.
- (6) (a) Zhang, B.; Clearfield, A. *J. Am. Chem. Soc.* **1997**, *119*, 2751. (b) Sharma, C. V. K.; Clearfield, A. *J. Am. Chem. Soc.* **2000**, *122*, 1558. (c) Sharma, C. V. K.; Clearfield, A. *J. Am. Chem. Soc.* **2000**, *122*, 4394. (d) Sharma, C. V. K.; Clearfield, A.; Cabeza, A.; Aranda, M. A. G.; Bruque, S. *J. Am. Chem. Soc.* **2001**, *123*, 2885. (e) Sharma, C. V. K.; Hessheimer, A. J.; Clearfield, A. *Polyhedron* **2001**, *20*, 2095.
- (7) (a) Kahn, O. *Molecular Magnetism*; VCH Publishers: New York, 1993. (b) Miller, J. S.; Buschmann, W. E. *Inorg. Chem.* **2000**, *39*, 2411. (c) Smith, J. A.; Galan Mascaros, J. R.; Clérac, R.; Dunbar, K. R. *Chem. Commun.* **2000**, 1077.

produce the low valence synthetic mineral hureaulite, $[\text{Mn}_5(\mu\text{-OH}_2)_2(\text{HPO}_4)_2(\text{H}_2\text{O})_2]$, **2**.⁸ These interesting results in the literature have prompted further investigations of the experimental conditions amenable for the synthesis of high- or low-valence Mn–phosphate complexes and a study of some of their structural and functional properties. Also, the fact that phosphate anions bridge metal centers with short metal–metal separation distances makes them very useful ligands for the design of novel network topologies for controlling magnetic properties.⁷

In this present work, the magnetic properties and oxidation state of the metal centers of two distinct Mn(II) complexes have been characterized. A two-dimensional layered structure, $[\text{Mn}(\text{HPO}_4)\cdot(\text{H}_2\text{O})_3]$, **1**, and a three-dimensional synthetic mineral, $[\text{Mn}_5(\mu\text{-OH}_2)_2(\text{HPO}_4)_2(\text{PO}_4)_2(\text{H}_2\text{O})_2]$, **2**, were isolated by reacting phosphoric acid with manganese salts under ambient and hydrothermal conditions. Furthermore, new synthetic routes used to obtain **1** and **2**, which have been previously prepared,⁹ are reported.

Experimental Section

Synthesis. $\text{Mn}(\text{O}_2\text{CCH}_3)_2\cdot 4\text{H}_2\text{O}$ (1.23 g, 5.0 mmol) and H_3PO_4 (0.98 g, 10.0 mmol) were dissolved in distilled deionized water (20.0 mL). Treating the resultant solution (pH = 3.3) using both solvent evaporation and hydrothermal techniques formed a crystalline solid phase. A clear solution was obtained by heating the above solution at 50 °C. Slow evaporation over a period of 3–4 days resulted in $[\text{Mn}(\text{HPO}_4)(\text{H}_2\text{O})_3]$, **1**, crystals (yield ca. 50%). However, when the same solution was placed in a Teflon-lined high-pressure vessel and heated in an oven at 120 °C for 36 h, a synthetic mineral, hureaulite, $[\text{Mn}_5(\mu\text{-OH}_2)_2(\text{HPO}_4)_2(\text{PO}_4)_2(\text{H}_2\text{O})_2]$, **2**, was formed. The final light pink crystalline product, **2**, was filtered and dried in an oven at 50 °C (yield 40%). When nitrilotri(methylphosphonic acid), $\text{N}(\text{CH}_2\text{PO}_3\text{H}_2)_3$ (2.0 gm, 5.0 mmol), was added to the above 1:2 mixture of Mn– H_3PO_4 under hydrothermal conditions, only the synthetic mineral **2** was formed. This triphosphonic acid did not form a complex with manganese under these conditions, but did so in the absence of the phosphonic acid.¹⁰ Furthermore, complexes **1** and **2** were found to form exclusively regardless of whether the molar ratios of manganese acetate/phosphoric acid molar ratios were 1:1 (pH = 4.0), 1:3 (pH = 2.6), or 1:4 (pH = 1.80). These results indicate that formations of **1** and **2** are a result of disproportionation reactions between $\text{Mn}(\text{CH}_3\text{CO}_2)_2\cdot 4\text{H}_2\text{O}$ and H_3PO_4 in aqueous media.

Characterization. TGA on **1** (22.52 mg) and **2** (30.97 mg) was performed using a Dupont Instrument 951 Thermogravimetric Analyzer under N_2 atmosphere. The samples were heated starting from ambient temperature to 1000 °C with a 5 °C/min heating ramp. The ion exchange properties of the synthetic mineral, **2**, and its dehydrated form, **2D** (obtained by heating **2** at 350 °C for 3 h), were studied in the presence of macro amounts of Na, Ca, ⁸⁹Sr,

and ¹³⁷Cs radioactive isotopes. The distribution coefficients (K_D) were determined using thoroughly grounded samples of **2** and **2D**. The powdered samples (0.01 g) were equilibrated with 20 mL of 0.01 M NaNO_3 , 0.01 M $\text{Ca}(\text{NO}_3)_2$, and deionized water containing trace amounts of ⁸⁹Sr and ¹³⁷Cs for 1 day at ambient temperature with constant rotary mixing. The solids were separated from solution by centrifugation and filtered through 0.22 μm Minispike PVDF Bulk Acrodisk 113 filters. The filtered samples (2 mL aliquots) were measured for ¹³⁷Cs and ⁸⁹Sr activities (cpm) by a liquid scintillation counter Wallac LKB 1217 Rackbeta. Na and Ca concentrations in the solution were measured by atomic absorption spectroscopy (AAS). The distribution coefficient (K_D) values were calculated according to:

$$K_D = \frac{\text{concentration in exchanger}}{\text{concentration in solution}} = \frac{(A_0 - A_{\text{eq}}) V}{A_{\text{eq}} m} \quad (1)$$

where A_0 and A_{eq} are the activities of the tracer initially and at equilibrium, and V/m is the solution volume to exchanger mass ratio (batch factor, mL g^{-1}). The pHs of the sample solutions were measured after equilibrium was established with the exchanger.

Magnetic susceptibility measurements were obtained with the use of a Quantum Design SQUID magnetometer MPMS-XL (housed in the Chemistry Department at Texas A&M University and in the Centre de Recherche Paul Pascal). Measurements were performed on finely ground crystalline samples of **1** (67.83 mg) and **2** (96.10 mg). The magnetic data were corrected for the sample holder and the diamagnetic contribution calculated from Pascal's constants.¹¹ XPS on **1**, **2**, and **2D** were performed in an ion-pumped (300 L/s) Perkin-Elmer PHI 560 system using a PHI 25-270AR double-pass cylindrical mirror analyzer. A Mg $K\alpha$ anode (photon energy $h\nu = 1253.6$ eV) was operated at 15 kV and 250 W. High-resolution scans were performed with 50 eV pass energy. Adventitious carbon for the C 1s orbital at a binding energy of 284.7 ± 0.2 eV was used to correct for sample charging. The system pressure during XPS analysis was ca. 1×10^{-8} Torr. The Cu $2p_{3/2}$ (932.7 eV) and Au $4f_{7/2}$ (84.0 eV) orbitals were used as standards from sputter-cleaned foils to calibrate the XPS binding energy (BE) range.¹² XRD data ($4 < \theta < 56$) on complexes **1** and **2** were collected on a Bruker-AXS CCD area detector-equipped diffractometer with Mo $K\alpha$ ($\lambda = 0.71073$ Å) radiation at 110 K using a stream of nitrogen gas. The crystal structures of **1** and **2** were solved by direct methods using the SHELXTL package.¹³ All the non-hydrogen atoms were anisotropically refined, and the OH protons were determined using difference Fourier maps, and their locations were verified by comparing the concerned P–O bond lengths and hydrogen-bonding distances. The crystallographic details of complexes **1** and **2** are summarized in Table 1.

Results and Discussion

$[\text{Mn}(\text{HPO}_4)(\text{H}_2\text{O})_3]$, **1.** X-ray crystallographic analysis of product **1** is in excellent agreement with those reported by Cudennec et al.⁹ In compound **1**, Mn(II) adopts an octahedral geometry and is coordinated by three water molecules and three oxygen atoms of the doubly deprotonated phosphoric acid. Compound **1** has a layered structure and is isomorphic to the natural mineral newberyite, $[\text{Mg}$ -

- (8) De Amorim, H. S., Jr.; Do Amaral, M. R.; Moreira, L. F.; Mattievich, M. E. *J. Mater. Sci. Lett.* **1996**, *15*, 1895.
 (9) (a) Cudennec, Y.; Riou, A.; Gerault, Y. *Acta Crystallogr.* **1989**, *C45*, 1411. (b) Gerault, P. Y.; Riou, A.; Cudennec, Y. *Acta Crystallogr.* **1985**, *C43*, 1829.
 (10) Recently we have shown that Mn(II) salts, $\text{MnSO}_4\cdot x\text{H}_2\text{O}$ or $\text{Mn}(\text{O}_2\text{-CCH}_3)_2\cdot 4\text{H}_2\text{O}$, along with several other transition(II) metal salts react with $\text{N}(\text{CH}_2\text{PO}_3\text{H}_2)_3$ under hydrothermal conditions to form isomorphous trihydrated metal–phosphonate complexes, $[\text{M}(\text{N}(\text{CH}_2\text{PO}_3\text{H}_2)_3)(\text{H}_2\text{O})_3]$, M = Mn, Co, Ni, Zn, Cu, or Cd. It is interesting to note that in the presence of phosphoric acid, $\text{N}(\text{CH}_2\text{PO}_3\text{H}_2)_3$ does not coordinate with manganese. See ref 6d.

- (11) *Theory and Applications of Molecular Paramagnetism*; Boudreaux, E. A., Mulay, L. N., Eds; John Wiley & Sons: New York, 1976.
 (12) Seah, M. P. *Surf. Interface Anal.* **1989**, *14*, 488.
 (13) Sheldrick, G. M. *SHELXTL*, Crystallographic Software Package, version 5.1; Bruker-AXS: Madison, Wisconsin, 1998.

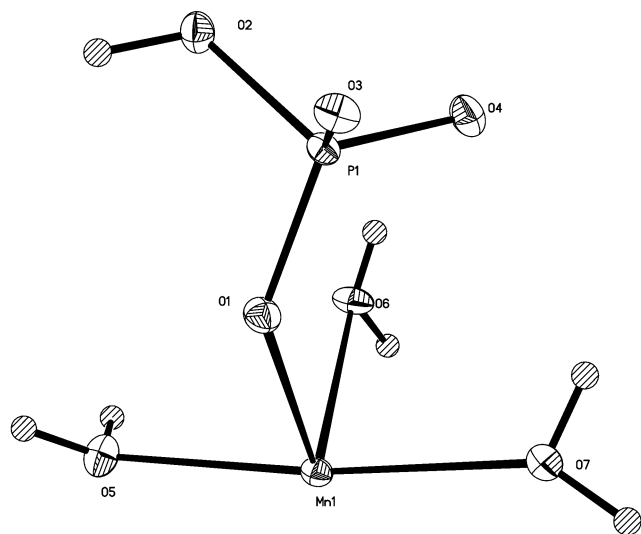


Figure 1. Two-dimensional layered structure of $\text{Mn}(\text{HPO}_4)\cdot 3\text{H}_2\text{O}$ (compound **1**).

$(\text{HPO}_4)(\text{H}_2\text{O})_3$.¹⁴ Mn(II) in **1** adopts an octahedral geometry and is coordinated by three water molecules and three oxygen atoms of the monohydrogenphosphate (Figure 1). The oxygen atoms of the doubly deprotonated phosphoric acid interconnect the metal centers to form a layered structure by sharing corners, as shown in Figure 2. The three water molecules are in a meridional disposition. The bond distances for Mn–O range from 2.102(2) to 2.222(2) Å with the three water O–Mn bonds on average being 3% larger than the

Table 1. Crystallographic Details of **1** and **2**

	color	colorless	light pink
formula		$\text{H}_7\text{MnO}_7\text{P}$	$\text{H}_{10}\text{Mn}_5\text{P}_4\text{O}_{20}$
M g/mol		204.97	728.65
cryst syst		orthorhombic	monoclinic
space group		<i>Pbca</i>	<i>C2/c</i>
<i>a</i> /Å		10.173(2)	17.591(2)
<i>b</i> /Å		10.423(2)	9.1236(9)
<i>c</i> /Å		10.786(2)	9.497(1)
α /deg		90	90
β /deg		90	96.471(2)
γ /deg		90	90
Z		8	4
<i>V</i> /Å ³		1143.7(3)	1514.5(3)
<i>d</i> /g cm ⁻³		2.381	3.196
measured reflns		6574	3322
unique reflns		1374	1083
$R1 > 2\sigma(I)$		0.0327	0.038
wR2		0.088	0.096
GOF		1.129	1.16

Mn–O phosphate bonds. The metal centers within the layer are separated by 5.08 and 5.50 Å in the *a* and *b* directions, respectively. The metal centers across the layer are separated by ca. 5.5 Å (Figure 3). As the layered structure of **1** is neutral and hydrophilic, it may function as a solid acid to intercalate neutral hydrophilic organic guest molecules.¹⁵ However, the two-dimensional layers are tightly held together by strong hydrogen bonds between water molecules and hydroxy groups of the doubly protonated phosphate (a total of nine intra- and intermolecular O–H \cdots O hydrogen bonds in the range of 2.6–3.0 Å were observed). The P1–O4 bond is significantly longer (1.591(1) Å) than the average (1.523–

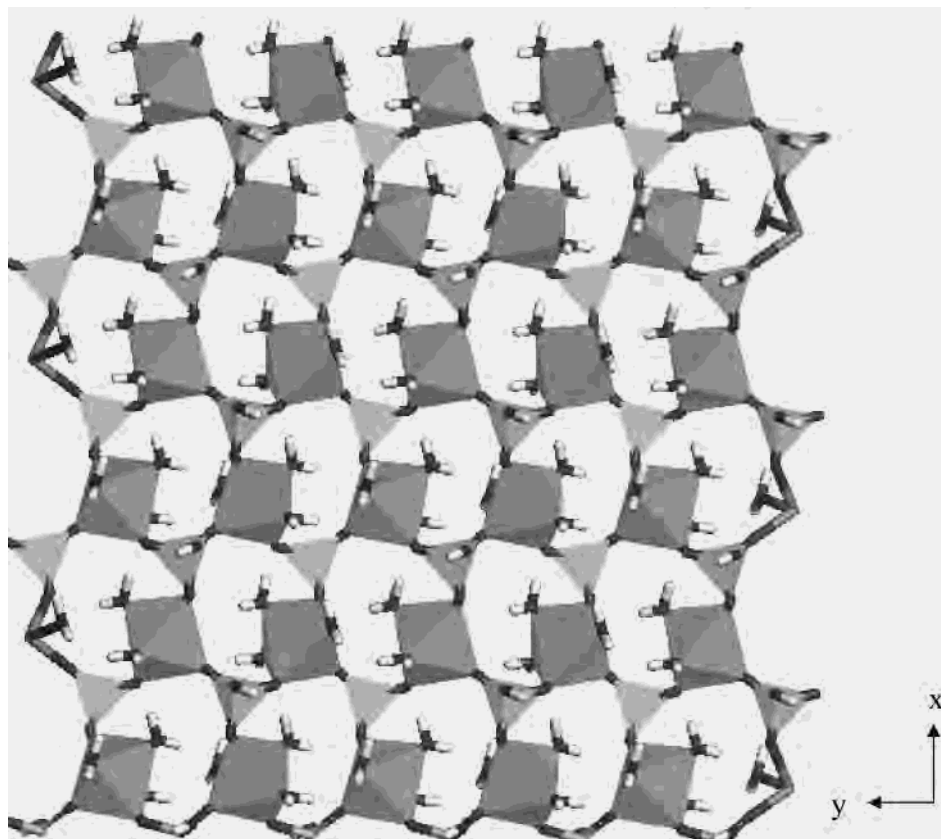


Figure 2. Polyhedral representation of the layers in compound **1** showing corner sharing between octahedra and tetrahedra.

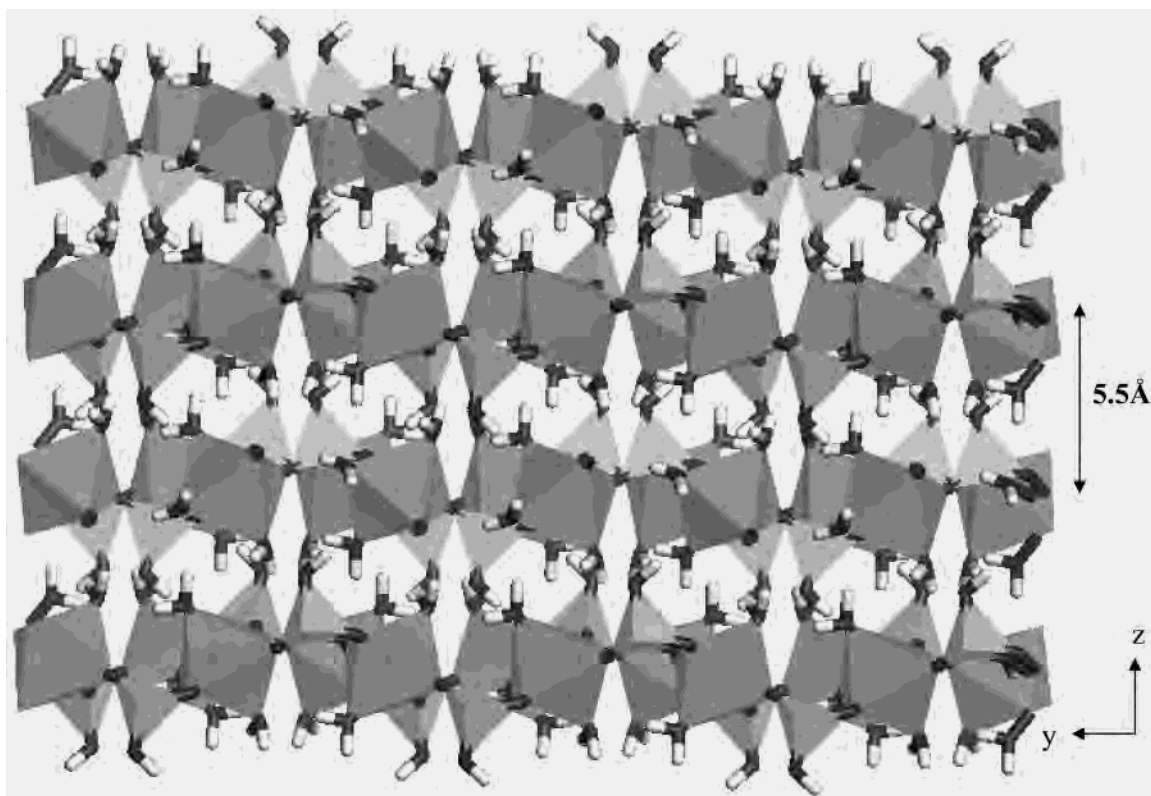


Figure 3. Stacking of layers in $\text{Mn}(\text{HPO}_4)\cdot 3\text{H}_2\text{O}$. The interlayer distance is $\sim 5.5 \text{ \AA}$.

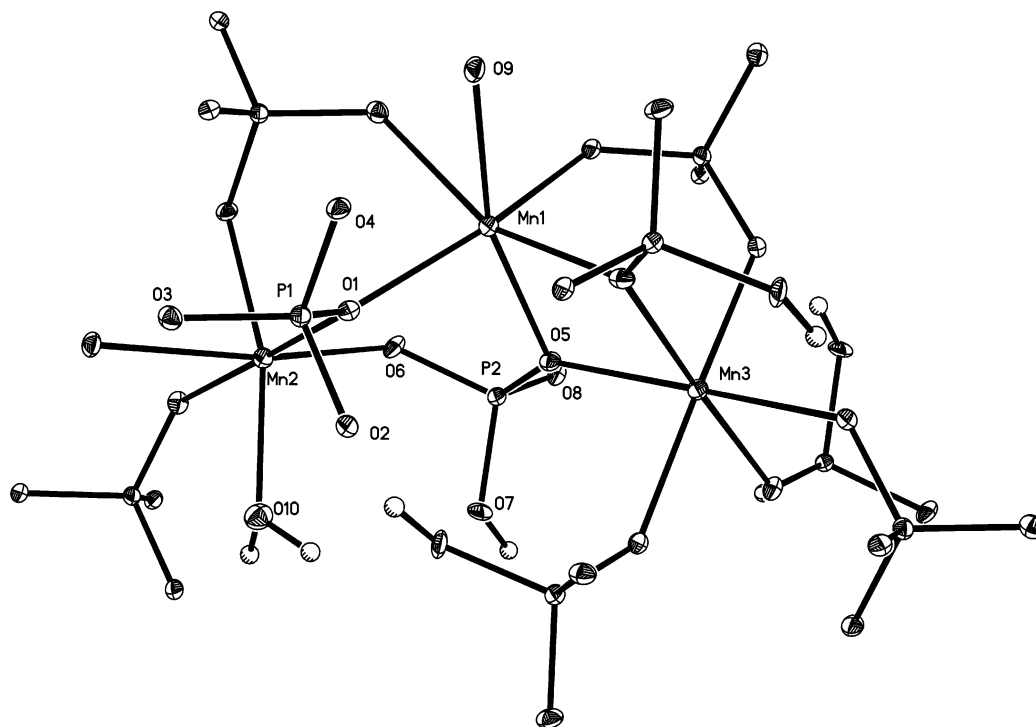


Figure 4. ORTEP drawing of a portion of compound **2** showing the connectivity of tetrahedra and octahedra.

(2) Å) of the other three phosphorus–oxygen bonds and bears the proton. TGA analysis of **1** showed that coordinated water molecules are lost completely at 375 °C.

$[\text{Mn}_5(\mu\text{-OH}_2)_2(\text{HPO}_4)_2(\text{PO}_4)_2(\text{OH}_2)]$. Compound **2** has a complex three-dimensional structure in which the cation metal centers are bridged by PO_4^{3-} , HPO_4^{2-} , and OH_2 groups. The diagram of **2** (Figure 4) shows the coordination environments of three crystallographically distinct Mn centers. Every metal cation interlinks the neighboring metal

(14) Abbona, F.; Boistelle, R.; Haser, R. *Acta Crystallogr.* **1979**, *B35*, 2514.

(15) Prevot, V.; Forano, C.; Besse, J. P.; Abraham, F. *Inorg. Chem.* **1998**, *37*, 4293.

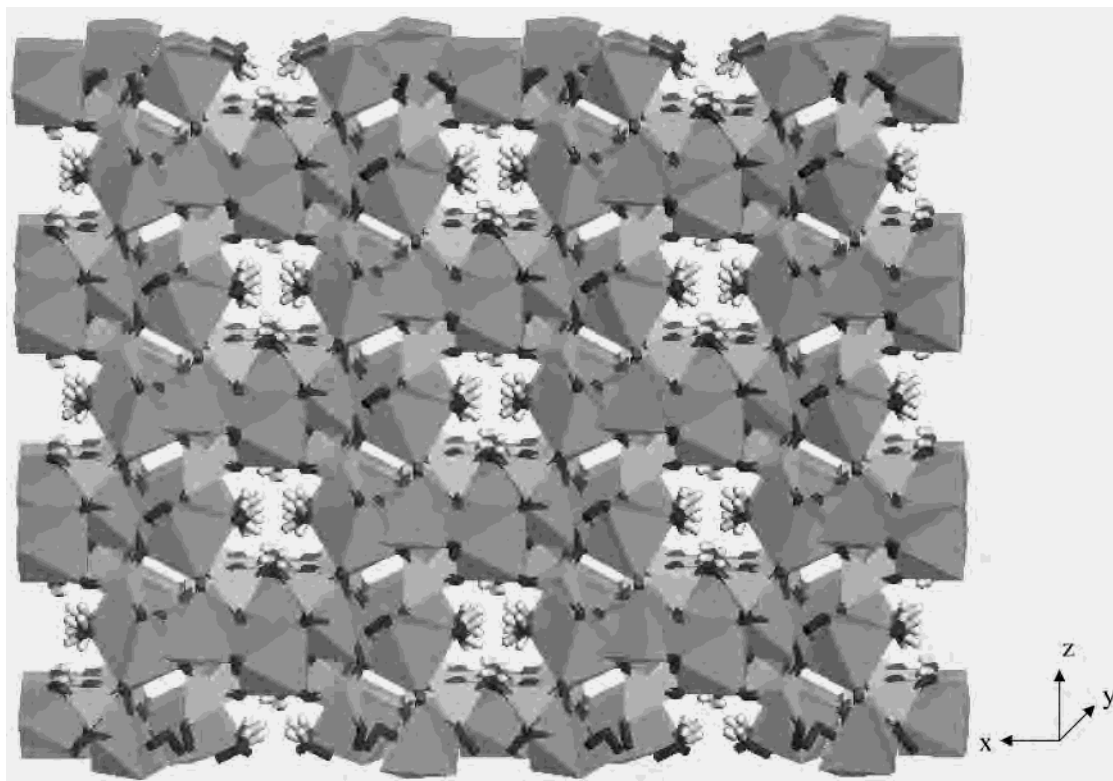


Figure 5. Complex three-dimensional architecture of **2**. The coordinated water molecule and OH group of a monohydrogen phosphate actively involved in hydrogen bonding, which does not bridge the metal centers.

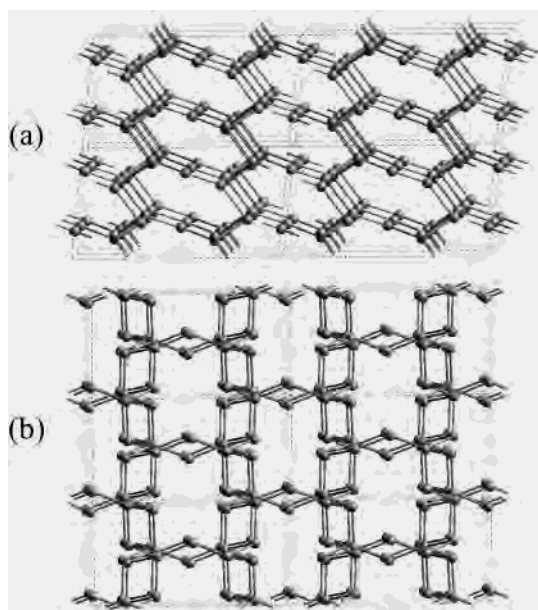
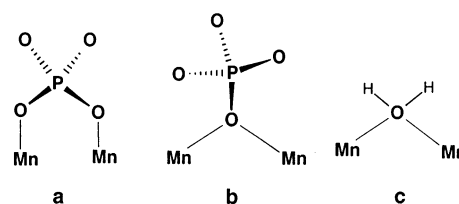


Figure 6. Simplified polygon network topology of compound **2**. (a) Viewed along the *ac* plane. (b) Viewed along the *ab* plane. For the sake of clarity, the coordinated functional groups are omitted. The metal centers are separated by less than 3.8 Å. Note that the metals are three-dimensionally disposed and form a polygon structure consisting of octagons and tetragons.

centers using any of the three types of bridging modes (Scheme 1).

The complex topology of metal–metal interaction network in **2** leads to a possible frustrated spin–spin coupling and glassy magnetic behavior (Figures 5 and 6). Although we have determined the H atom positions of the water molecules from a difference Fourier, the possibility that manganese salts

Scheme 1



can adopt mixed valence states in their metal complexes using oxo- or hydroxy bridges prompted us to carry out XPS studies to verify the oxidation state of Mn. The presence of three crystallographically independent Mn atoms in the asymmetric unit of **2** further complicates the determination of the Mn oxidation state from the crystallographic studies. Compound **2** is shown to have a very complex three-dimensional structure, in which every metal cation interlinks the neighboring metal centers using any of the three types of bridging modes shown in Scheme 1. The hydroxyl group of HOPO_3^{2-} , labeled P2–O7, and coordinate water molecules (bridging and terminal) actively participate in hydrogen bonding (five unique O–H \cdots O contacts in the range of 2.6–2.8 Å were observed). The complexity of the three-dimensional network and distorted octahedral metal environment in **2** makes it difficult to visualize the nature of metal–metal interactions and the network topology (Figure 5). Therefore, we have decided to simplify the structural features of **2** by omitting ligands and representing the metal centers as nodes to highlight their 3D connectivity. Figure 6 represents a polygon structure made of octagons and squares, where the metal–metal separation distances are in the range of 3.30–3.80 Å. It is worth noticing that this complex three-

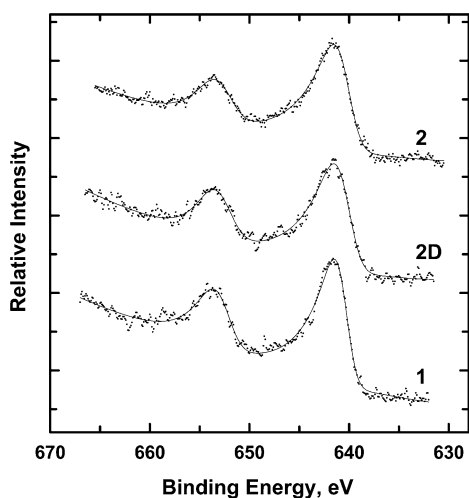


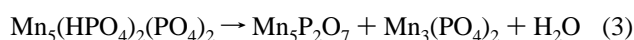
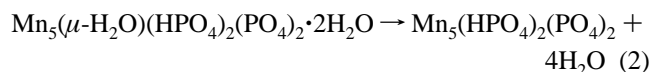
Figure 7. Mn $2p$ XPS core levels of **1**, **2**, and **2D**.

dimensional architecture leads to a complicated network of magnetic interactions and to possible magnetic frustration (vide infra).

XPS (along with the pink color of the solid) confirms that the Mn atoms in compounds **1**, **2**, and **2D** have +2 oxidation state and the metal centers are bridged by neutral water molecules and not by hydroxyl or oxo groups. The Mn $2p_{3/2}$ core level shift of **1** is identical to both of those of **2** and **2D** (Figure 7) at BE = 641.5 eV, which matches the literature values of Mn(II) oxidation states of MnO.¹⁶ The BEs of the $2p_{3/2}$ orbitals in the dehydrated form of compound **2** remain unchanged, and the XPS peak shapes of the dehydrated sample almost overlap with those of **2**, indicating that the dehydration does not alter the oxidation state of **2**. The similarity between the XPS spectra of compounds **1** and **2** revealed that the Mn in both compounds unambiguously exists in +2 oxidation state and both compounds **1** and **2** have the same coordination environment.

TGA weight loss curves for compounds **1** and **2** are shown in Figure 8. The loss of water of compound **1** began at 70 °C with a change in slope of the curve at 138 °C. The weight loss over this temperature is 22.5%, equivalent to the loss of 2.56 mol of water. Over the temperature range 138–358 °C, compound **1** lost additional 7.5% weight, or 0.85 mol of water, making a total of 3.41 mol compared to 3.5 mol required by the proposed formula.

Compound **2** exhibits two weight losses. The first occurred over the temperature range 365–480 °C, with a 2.4% weight loss. The second weight loss was barely within the limits of detection. The two reactions can be represented as:



Ion exchange experiments were carried out on **2** and on its dehydrated phase, **2D**, to measure the availability of the

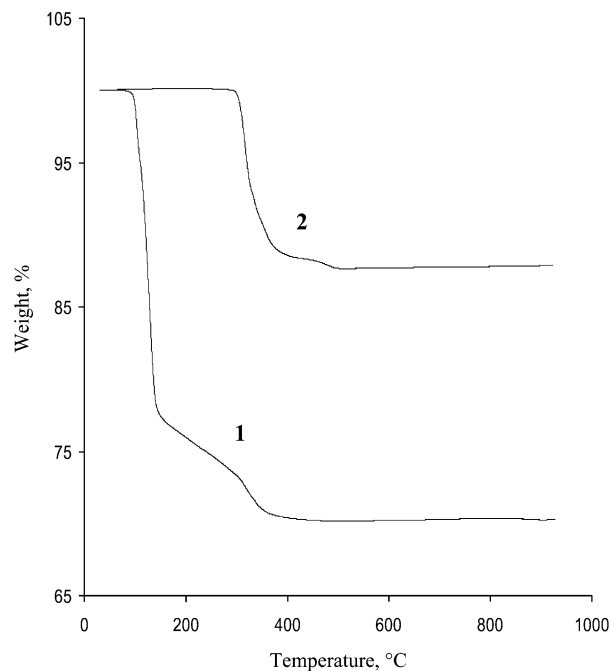


Figure 8. Thermogravimetric weight loss curves for compounds **1** and **2**.

acidic protons of **2**. Neutralization was performed via replacement of the acidic protons with cations without changing the three-dimensional architecture of **2**. Ion exchange experiments were carried out in the presence of macro amounts of Na and Ca metal cations and radiotracers ^{137}Cs and ^{89}Sr . The results of the ion exchange experiments are summarized in Table 2. As seen from the results (Table 1), the dehydrated sample acts more readily as an ion exchanger than the hydrated sample, **2**. For example, at neutral pH, the uptakes of ^{137}Cs and ^{89}Sr by **2D** are far greater than by **2**, with the uptake of ^{89}Sr being particularly high. Also, both hydrated and dehydrated samples seem to prefer Na^+ over Ca^{2+} . It was observed in the competitive ion exchange experiments with **2D** that in the presence of macro amounts of sodium the uptake of both trace ions ^{137}Cs and ^{89}Sr decreased significantly. This decrease in uptake of the isotopes may be attributed to the fact that the material is more selective for sodium than the larger Cs and Sr cations. Na^+ cations, because of their smaller size, rapidly entered into the open cavities of **2D** along with water molecules and blocked the cavity entrances for diffusion of ^{137}Cs or ^{89}Sr ions. When the ion exchange experiments were carried out on a sample and first treated to temperatures above 500 °C, the uptake of both ^{137}Cs or ^{89}Sr decreased to negligible values. Compounds **2** and **2D** are not particularly good ion exchangers due to their small pore size and lack of access to the crystal interior.

The magnetic properties of both **1** and **2** were measured in detail to determine the correlation between the bridging modes of phosphates in magnetically active metal phosphates. Previously measured magnetic properties of **2** revealed ferromagnetic behavior.¹⁷ However, our reexamination of the magnetic properties of **2** shows that complex **2** is

(16) (a) Carver, J. C.; Schweitzer, G. K. *J. Chem. Phys.* **1972**, *57*, 973–982. (b) Strohmeier, B. R.; Hercules, D. M. *J. Phys. Chem.* **1984**, *88*, 4922.

(17) Domingues, P. H.; Moreira, L. F.; Mattievich, E.; Sarkissian, B. *J. Magn. Magn. Mater.* **1997**, *167*, 87–92.

Table 2. Ion Exchange Properties of **2** and Its Dehydrate, **2D**^a

sample	0.01 M NaNO ₃	0.01 M Ca(NO ₃) ₂	deionized water/ ¹³⁷ Cs	deionized water/ ⁸⁹ Sr	0.1 M NaNO ₃ + ¹³⁷ Cs	0.1 M NaNO ₃ + ⁸⁹ Sr
2	98 (6.90) ^b	9.5 (6.80)	2.1 (6.34)	12 (6.28)	6.5 (6.54)	2 (6.80)
2D	200 (6.85)	36 (6.56)	200 (6.83)	1000 (6.84)	9.5 (6.81)	84 (6.16)
2N			31 (6.43)	84 (6.16)		

^a Distribution coefficients ($K_D/\text{mL g}^{-1}$) for Na⁺, Ca²⁺, ¹³⁷Cs, and ⁸⁹Sr. ^b Values in parentheses refer to pH.

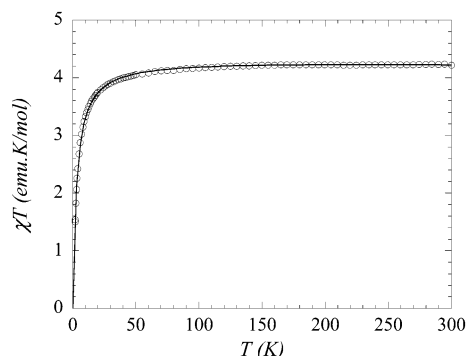


Figure 9. Temperature dependence of the product χT for **1** at 1000 G. The solid line represents the Curie–Weiss fit to the data with $C = 4.3 \text{ emu}\cdot\text{K/mol}$ and $\theta = -3.2 \text{ K}$.

not a true ferromagnetic material but, in fact, a glassy magnet.¹⁸ Compound **1** reveals a Curie–Weiss behavior in the whole range of temperatures studied (1.8–300 K, Figure 9). The presence of Mn(II) with a $S = 5/2$ magnetic spin is confirmed by a Curie constant of $4.3 \text{ emu}\cdot\text{K/mol}$ (4.375 is expected for a $S = 5/2$ magnetic spin and $g = 2$). As shown in Figure 9, the χT product is fairly stable between 300 and 80 K at $4.2 \text{ emu}\cdot\text{K/mol}$ and decreases below 80 K to reach a value of $1.5 \text{ emu}\cdot\text{K/mol}$ at 1.8 K. This behavior is clearly indicative of dominating antiferromagnetic interactions between the Mn^{II} magnetic centers, which can be quantified by a negative Weiss constant of -3.2 K . An organic–inorganic compound, $\text{VO}_6\text{H}_3\text{PO}_3\cdot 2\text{H}_2\text{O}$, also has the new-beryite structure.¹⁹ This vanadium compound is orthorhombic, $a = 10.03$, $b = 9.69$, $c = 9.77 \text{ \AA}$ with the b -axis being the interlayer spacing. The layers are formed from $(\text{VO})\text{O}_3\text{P}(\text{H}_2\text{O})_2$ octahedra with pendant phenyl rings. Normally, the noninterpenetrating phenyl groups would require an interlayer spacing of $\sim 14 \text{ \AA}$ as in $\text{VO}(\text{C}_6\text{H}_5\text{O}_3)(\text{H}_2\text{O})$.²⁰ A much smaller spacing was observed for $\text{VO}_6\text{H}_3\text{PO}_3\cdot 2\text{H}_2\text{O}$; nevertheless, magnetic measurements revealed a Curie behavior down to 4 K. The vanadyl oxygen takes the place of one water molecule in the vanadium coordination sphere and at the same time, is responsible for the $\text{V}/\text{C}_6\text{H}_5\text{PO}_3$ ratio of one. As a result, the layer arrangement in $\text{Mn}(\text{HPO}_4)\cdot$

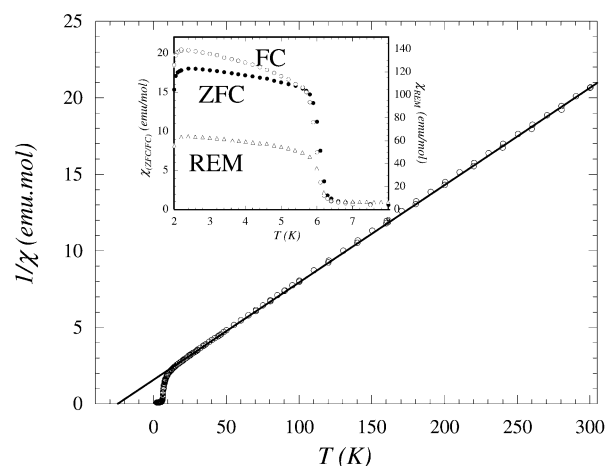


Figure 10. Temperature dependence of $1/\chi$ for **2** at 200 G from 2 to 300 K. Inset: temperature dependence of zero-field cooled (ZFC) and field cooled (FC) susceptibilities in 10 G applied field and remanent (REM) magnetization after cooling in 200 G and measuring in 0.1 G.

$3\text{H}_2\text{O}$ and the vanadyl phenylphosphonate dihydrate are quite similar, accounting for the similarity in their magnetic behavior.

The plot of $1/\chi$ versus T for **2**, presented in Figure 10 reveals that in the high-temperature regime ($T > 30 \text{ K}$), the magnetic data exhibit Curie–Weiss behavior (with Curie and Weiss constants of $16 \text{ emu}\cdot\text{K/mol}$ and -26 K , respectively). The Curie constant obtained experimentally is low as compared to the spin-only value of $21.9 \text{ emu}\cdot\text{K/mol}$ for five Mn(II), $S = 5/2$, and a Landé factor of 2. The origin of the low Curie constant is not well understood.¹⁷ In this material, the Weiss constant ($\theta = -26 \text{ K}$) clearly indicates that dominant magnetic interactions in **2** are also antiferromagnetic. As shown in Figure 10, below 6.2 K, the ZFC, FC, and REM experiments reveal the presence of a spontaneous magnetization. Figure 11 shows the field dependence of the magnetization at 2 K, where no coercivity is observed. It is worth noticing that the magnetic moment does not saturate even at 7 T. This lack of saturation even at high fields is indicative of some degree of spin canting probably resulting from the complicated network of magnetic interactions and magnetic anisotropy.^{21,22}

The existence of spontaneous magnetization below 6.2 K is also confirmed by the ac measurements in zero-dc field,

- (18) (a) Clérac, R.; O’Kane, S.; Cowen, J.; Ouyang, X.; Heintz, R.; Zhao, H.; Bazile, M. J.; Dunbar, K. R. *Chem. Mater.* **2003**, *15*, 1840. (b) Kaul, B. B.; Durfee, W. S.; Yee, G. T. *J. Am. Chem. Soc.* **1999**, *121*, 6862. (c) Buschmann, W. E.; Enslin, J.; Gutlich, P.; Miller, J. S. *Chem.–Eur. J.* **1999**, *5* (10), 3019. (d) Wynn, C. M.; Albercht, A. S.; Landee, C. P.; Navas, C.; Turnbull, M. M. *Mol. Cryst. Liq. Cryst. Sci. Technol., Sect. A* **1995**, *274*, 657. (e) Buschmann, W. E.; Miller, J. S. *Inorg. Chem.* **2000**, *39*, 2411. (f) Cava, R. J.; Ramirez, A. P.; Huang, Q.; Krajewski, J. J. *J. Solid State Chem.* **1998**, *140*, 337. (g) Sellers, S. P.; Korte, B. B.; Fitzgerald, J. P.; Reiff, W. M.; Yee, G. T. *J. Am. Chem. Soc.* **1998**, *120*, 4662.
- (19) Johnson, J. W.; Jacobson, A. J.; Brodly, J. F.; Lewandowski, J. T. *Inorg. Chem.* **1984**, *23*, 3842.
- (20) Haun, G.; Jacobson, A. J.; Johnson, J. W.; Corcoran, E. W., Jr. *Chem. Mater.* **1990**, *2*, 91.

- (21) (a) Morrish, A. H. *The Physical Principles of Magnetism*; John Wiley & Sons: New York, 1965; p 510. (b) Jacobs, I. S. *J. Phys. Chem. Solids* **1959**, *11*, 1. (c) Jacobs, I. S. *J. Phys. Chem. Solids* **1960**, *15*, 54.
- (22) (a) Conklin, B. J.; Sellers, S. P.; Fitzgerald, J. P.; Yee, G. T. *Adv. Mater.* **1994**, *11*, 836. (b) Bellitto, C.; Federici, F.; Colapietro, M.; Portalone, G.; Caschera, D. *Inorg. Chem.* **2002**, *41*, 709. (c) Gao, E.-Q.; Wang, Z.-M.; Yan, C.-H. *Chem. Commun.* **2003**, 1748. (d) Rodríguez-Martín, Y.; Hernández-Molina, M.; Sanchiz, J.; Ruiz-Pérez, C.; Lloret, F.; Julve, M. *J. Chem. Soc., Dalton Trans.* **2003**, 2359.

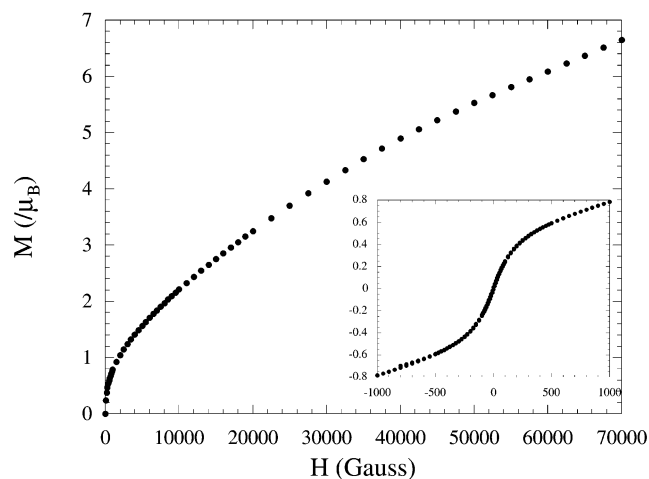


Figure 11. Field dependence of the first magnetization for **2** at 2 K up to 7 T. Inset: Field hysteresis loop at 2 K between -1000 and 1000 G.

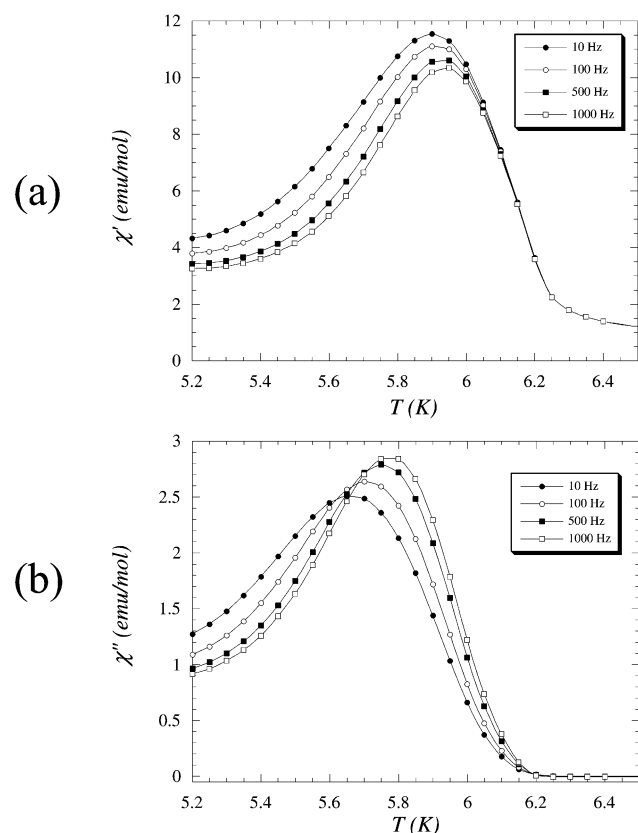


Figure 12. Temperature dependence of the ac susceptibilities (a) in-phase and (b) out-of-phase at different frequencies from 10 to 1000 Hz in zero dc field.

which reveal both in-phase and out-of-phase signals. The ac susceptibilities are slightly dependent on the frequency of the alternating field. The position of the maximum of the χ' and χ'' peaks increase by 0.05 and 0.112 K, respectively, when the ac frequency is increased from 10 to 1000 Hz (Figure 12). This behavior is not expected for true three-dimensionally ordered magnets, but is a signature of a glassy effect (spin-glass-like) or superparamagnetism.^{18,23–25} To help experimentalists interpret observed behavior, J. A. Mydosh introduced the concept of the frequency shift parameter, γ , which is defined by the slope of T_f vs $\log(\nu)$, normalized at

$T_f(0)$, where T_f is the “freezing” temperature at the peak maximum (in χ' at each frequency), and $\log(\nu)$ is the logarithm of the ac frequency.^{18,23} The calculated γ for **2** is found to be 0.003 and consistent with the spin-glass-like behavior.²³ Generally, glassiness can result from two main origins: (i) randomness (atom or bond disorder or defects in the crystal structure) and (ii) competing ferro- and antiferromagnetic interactions.^{23,24,26} Although either phenomenon can lead to glassy behavior, in most cases, both of them are operative. In the case of compound **2**, the glassiness seems to be mainly a result of competing magnetic interactions due to the complexity of the network topology (for examples, see the pyrochlore or jarosite families²⁷).

In summary, varying experimental conditions play an important role in the synthesis of manganese–phosphates. While the room-temperature synthesis of manganese–phosphates in aqueous media results in a layered material, the hydrothermal conditions result in a synthetic mineral, hueraulite, **2**. The neutral-layered coordination polymeric structure of **1** makes it a potential candidate for the intercalation of neutral hydrophilic organic molecules and may complement

- (23) (a) Mydosh, J. A. *Spin Glasses: An Experimental Introduction*; Taylor & Francis: London, 1993; p 64. (b) Chowdhury, D. *Spin Glasses and Other Frustrated Systems*; Princeton University Press: New Jersey, 1986. (c) Moorjani, K.; Coey, J. M. D. *Magnetic Glasses*; Elsevier: New York, 1984. (d) Binder, K.; Young, A. P. *Rev. Mod. Phys.* **1986**, *58* (4), 801. (e) O'Connor, C. J. *Research Frontiers in Magnetochemistry*; O'Connor, C. J., Ed.; World Scientific: London, 1993; p 109. (f) Ramirez, A. P. *Annu. Rev. Mater. Sci.* **1994**, *24*, 453.
- (24) (a) Sommer, R. D.; Korte, B. J.; Sellers, S. P.; Yee, G. T. *Mater. Res. Soc. Symp. Proc.* **1998**, *488*, 471. (b) Sellers, S. P.; Korte, B. B.; Fitzgerald, J. P.; Reiff, W. M.; Yee, G. T. *J. Am. Chem. Soc.* **1998**, *120*, 19, 4662. (c) Kaul, B. B.; Durfee, W. S.; Yee, G. T. *J. Am. Chem. Soc.* **1999**, *121*, 6862. (d) Bushmann, W. E.; Ensling, J.; Gütlich, P.; Müller, J. S. *Chem.–Eur. J.* **1999**, *5* (10), 3019. (e) Wynn, C. M.; Albrecht, A. S.; Landee, C. P.; Navas, C.; Turnbull, M. M. *Mol. Cryst. Liq. Cryst. Sci. Technol., Sect. A* **1995**, *274*, 657. (f) Landee, C. P.; Wynn, C. M.; Albrecht, A. S.; Zhang, W.; Vunni, G. B.; Parent, J. L.; Navas, C.; Turnbull, M. M. *J. Appl. Phys.* **1994**, *75*, 5535. (g) Bushmann, W. E.; Müller, J. S. *Inorg. Chem.* **2000**, *39*, 2411. (h) Brandon, E. J.; Rittenberg, D. K.; Arif, A. M.; Miller, J. S. *Inorg. Chem.* **1998**, *37*, 3376. (i) Brandon, E. J.; Arif, A. M.; Burkhart, B. M.; Müller, J. S. *Inorg. Chem.* **1998**, *37*, 2792. (j) Cava, R. J.; Ramirez, A. P.; Huang, Q.; Krajewski, J. J. *J. Solid. State Chem.* **1998**, *140*, 337.
- (25) In fact, the notation “spin-glass” usually refers to dilute systems such as Cu:Mn, and we prefer to use the term “glassy magnet” for **2**.
- (26) (a) Kahn, O. *Chem. Phys. Lett.* **1997**, *265*, 109. (b) Ramirez, A. P.; Espinosa, G. P.; Cooper, A. S. *Phys. Rev. Lett.* **1990**, *64* (17), 2070. (c) Walton, D.; McCleary, A.; Stager, C. V.; Raju, N. P. *Phys. Rev. B* **1999**, *59* (1), 135. (d) Harris, M. J.; Bramwell, S. T.; McMorrow, D. F.; Zeiske, T.; Godfrey, K. W. *Phys. Rev. Lett.* **1997**, *79* (13), 2554. (e) Gardner, J. S.; Dunsiger, S. R.; Gaulin, B. D.; Gingras, M. J. P.; Greedan, J. E.; Kiefl, R. F.; Lumsden, M. D.; MacFarlane, W. A.; Raju, N. P.; Sonier, J. E.; Swainson, I.; Tun, Z. *Phys. Rev. Lett.* **1999**, *82* (5), 1012. (f) Gardner, J. S.; Gaulin, B. D.; Lee, S.-H.; Broholm, C.; Raju, N. P.; Greedan, J. E. *Phys. Rev. Lett.* **1999**, *83* (1), 211. (g) Gingras, M. J. P.; Stager, C. V.; Raju, N. P.; Gaulin, B. D.; Greedan, J. E. *Phys. Rev. Lett.* **1997**, *78* (5), 947. (h) de Almeida, J. R. L. *Eur. Phys. J. B*, **2000**, *13*, 289.
- (27) (a) Ortega, I. J.; Puche, R. S.; de Paz, J. R.; Martinez, J. L. *J. Mater. Chem.* **1999**, *9*, 525. (b) Harris, M. J.; Bramwell, S. T.; McMorrow, D. F.; Zeiske, T.; Godfrey, K. W. *Phys. Rev. Lett.* **1997**, *79*, 2554. (c) Taira, N.; Wakeshima, M.; Hinatsu, Y. *J. Phys.: Condens. Matter* **1999**, *11*, 6983. (d) Raju, N. P.; Dion, M.; Gingras, M. J.; Mason, T. E.; Greedan, J. E. *Phys. Rev. B* **1999**, *59*, 14489. (e) Reimers, J. N.; Greedan, J. E.; Kremer, R. K.; Gmelin, E.; Subramanian, M. A. *Phys. Rev. B* **1991**, *43*, 3387. (f) Bramwell, S. T.; Harris, M. J. *J. Phys.: Condens. Matter* **1998**, *10*, L215. (g) Townsend, M. G.; Longworth, G.; Roudaut, E. *Phys. Rev. B* **1986**, *33*, 4919.

the positively charged, layered double hydroxides. Although the intercalation properties of this class of materials were not targeted in this study, they may be of significant importance in designing organic–inorganic hybrid materials with multifunctional properties.

The structural features of **2**, along with TGA, XPS, and magnetic studies, show that the Mn in this complex exists in the +2 oxidation state with neutral water molecules functioning as bridging units. Acidic protons of **2** are exchangeable with alkali and alkaline earth metals, and the exchange rate of protons with the metal cations can be accelerated/facilitated by removal of the coordinated water molecules. Our studies indicate that phosphoric acids do not promote the formation of high valence metal complexes in aqueous media (pH 2.0–4.0). Additional experimental factors for the stabilization of high valence manganese complexes need to be considered. The metal centers in complex **2** are

positioned at the corners of the octagons and squares and result in the formation of a glassy magnet, which has a spontaneous magnetization below 6.2 K and is a rare example of a glassy magnet crystal. It would seem that the competing magnetic interactions in the crystalline solid imposes the glassy magnetic nature to the material.

Acknowledgment. C.V.K.S., T.M., and A.C. would like to acknowledge the support received from NSF to carry out this work (Grant No. DMR9707151) and for the purchase of a Bruker-AXS SMART CCD area detector (Grant CHE-98 07975). R.C. would like to thank the CNRS, the University of Bordeaux I, the Institut Universitaire de Technologie de Bordeaux, and the Conseil Regional d'Aquitaine for financial support.

IC0300520